

# Stack Sizing for Optimal Current Drivability in Subthreshold Circuits

John Keane, Hanyong Eom, Tae-Hyoung Kim,  
Sachin Sapatnekar, and Chris Kim

**Abstract**—Subthreshold circuit designs have been demonstrated to be a successful alternative when ultra-low power consumption is paramount. However, the characteristics of MOS transistors in the subthreshold region are significantly different from those in strong-inversion. This presents new challenges in design optimization—particularly in complex gates with stacks of transistors. In this paper, we present a framework for choosing the optimal transistor stack sizing factors in terms of current drivability for subthreshold designs. We derive a closed-form solution for the correct sizing of transistors in a stack, both in relation to other transistors in the stack, and to a single device with equivalent current drivability. Simulation results show that our framework provides a performance benefit ranging up to more than 10% in certain critical paths.

**Index Terms**—Subthreshold logic, logical effort, ultra low power design

## I. INTRODUCTION

Due to the robust nature of static CMOS logic, circuits in this technology family can operate with supply voltages below the transistor threshold voltage ( $V_{th}$ ), while consuming orders of magnitude less power than in the normal strong-inversion region. The operating frequency of subthreshold logic is much lower than that of regular strong-inversion circuits ( $V_{dd} > V_{th}$ ) due to the small transistor current, which consists entirely of leakage current. The low operating frequency and low supply voltage combine to reduce both dynamic and leakage power, leading to the significant power savings seen in subthreshold designs.

Subthreshold logic holds promise for the growing number of applications in which minimal power consumption is the primary design constraint. Such circuits have received much attention in recent research, and a number of successful designs have been demonstrated. A multiplexer-based SRAM was proposed for subthreshold operation by the authors of [1]. They also introduced new tiny-XOR circuits and demonstrated their performance in a Fast Fourier Transform processor running at a supply voltage of 180mV. The authors of [2] presented a new high-density SRAM system operating down to 200mV at ISSCC 2007. In [3], Kim et al. built an ultra low power adaptive filter for hearing aid applications using subthreshold logic. Subthreshold-friendly logic styles and massively parallel DSP architectures were used in that work to achieve low voltage operation

The characteristics of MOS transistors in the subthreshold region are significantly different from those in the strong-inversion region. The saturation current, which was a near-linear function of the gate and threshold voltages in the strong-inversion region, becomes an exponential function of those values in the subthreshold regime [4]. In this work, we show that the

sizing methods used to obtain maximum performance must be reformulated for use in subthreshold designs due to these different characteristics. In particular, we present a framework for choosing the optimal transistor stack sizing factors in terms of current drivability for subthreshold circuits. A closed-form solution for the optimal sizing of stacked transistors is derived and shown to match simulation results. Our theoretical sizing values closely match those found in simulations with Predictive Technology Model (PTM) [5,6] devices ranging from 130nm technology down to the 45nm node. This sizing method is shown to provide a clear benefit in logic paths containing a large number of stacks where the nodal capacitance is not dominated by the increased device sizes used in our method.

## II. OPTIMAL 2-STACK SIZING

### A. Optimal Ratio between 2 Stacked Devices

The first step we take in developing the subthreshold stack sizing framework is finding the optimal width ratio between transistors in a stack for maximum drive current. Here we will present a closed-form expression for the relative sizing of two transistors in a stack, showing that it is beneficial to size up the transistor nearest to the supply rail ( $V_{dd}$  for PMOS, ground for NMOS). The starting point is the following pair of current equations for upper and lower transistors as situated in an NMOS stack (so the lower device is connected to ground), excluding the common factors that will cancel out when they are equated:

$$I_U = W_U e^{\frac{(V_{dd}-V_X)-(V_{t0}+\gamma V_X+\lambda_d(V_{dd}-V_X))}{mV_T}} \left(1 - e^{-\frac{(V_{dd}-V_X)}{V_T}}\right) \quad (1)$$

$$\approx W_U e^{\frac{(V_{dd}-V_X)-(V_{t0}+\gamma V_X+\lambda_d(V_{dd}-V_X))}{mV_T}} \\ I_L = W_L e^{\frac{V_{dd}-(V_{t0}+\lambda_d V_X)}{mV_T}} \left(1 - e^{-\frac{V_X}{V_T}}\right) \quad (2)$$

Here,  $W_U$  and  $W_L$  denote the upper and lower transistor widths, respectively, and  $V_X$  denotes the voltage at the node between those devices. The Drain-Induced Barrier Lowering (DIBL) coefficient (a negative number) is represented by  $\lambda_d$ , and  $\gamma$  is the body effect coefficient. The thermal voltage is represented by  $V_T$ , while  $V_{t0}$  stands for the nominal threshold voltage. According to simulation results,  $V_X \approx 10\%$  of  $V_{dd}$ . Each  $V_X$  term multiplied by the small DIBL coefficient (ranging from roughly -0.01 to -0.2 in current bulk technologies) can then be approximated as  $\sim 0$ . Moreover, note that  $e^{-(V_{dd}-V_X)/V_T} \approx 0$ . We use the symbol

$$\alpha = e^{\frac{-\lambda_d V_{dd}}{mV_T}}, \quad (3)$$

as well as the fact that  $m = 1 + \gamma$ , to further simplify calculations. Rewriting the two current equations and equating them yields the following relationship:

$$\alpha W_U e^{\frac{-V_X}{V_T}} = W_L \left(1 - e^{-\frac{V_X}{V_T}}\right) \quad (4)$$

Solving for  $V_X$  and using the definition  $V_T = kT/q$  gives us

$$V_X = \frac{kT}{q} \ln \left(1 + \frac{\alpha W_U}{W_L}\right) \quad (5)$$

We then define  $W_T = W_U + W_L$  to eliminate  $W_L$ , which results in the following current equation:

$$I_U = I_L = \frac{\alpha W_U (W_T - W_U)}{\alpha W_U + W_T - W_U} e^{\frac{V_{dd}-V_{t0}}{mV_T}} \quad (6)$$

Manuscript received October 22, 2006; revised March 16, 2007.

The authors are with the Department of Electrical and Computer Engineering at the University of Minnesota, Minneapolis, MN 55455 (email: {jkeane, eomxx001, thkim, sachin, chriskim}@ece.umn.edu)

Digital Object Identifier .....

We find the optimal size for  $W_U$  by setting  $(\partial I_U / \partial W_U)$  equal to zero. Again using our definition of  $W_T$ , we then find the optimal size for  $W_L$ . This derivation results in the following equations:

$$W_U = \frac{W_T}{1 + \sqrt{\alpha}} \quad (7)$$

$$W_L = \frac{W_T}{1 + \sqrt{\alpha}} \sqrt{\alpha} \quad (8)$$

According to these results, we expect to drive a higher current through the two-transistor stack when the lower device is larger than the upper transistor by a factor of  $\sqrt{\alpha}$ . For example, with an NMOS stack in 90nm PTM technology, when using a  $W_U$  of  $1\mu\text{m}$ , the optimal  $W_L$  would be  $1.23\mu\text{m}$  at  $V_{dd} = 0.2\text{V}$ , and  $1.30\mu\text{m}$  at  $V_{dd} = 0.3\text{V}$ . As shown in equation (3),  $\alpha$  is a function of  $V_{dd}$ , resulting in the different optimal width ratios for different  $V_{dd}$  values.

HSPICE simulations using 45nm through 130nm PTM technology files closely match the results of our derivation, and verify that the benefit of using the  $\sqrt{\alpha}$  sizing ratio is more pronounced for larger  $\alpha$  values (i.e., when the supply voltage is larger). PMOS transistor stacks exhibited the same sizing trends—optimal sizing requires the upper transistor (adjacent to the power supply) to be sized up by a factor of  $\sim\sqrt{\alpha}$ . Results for 90nm technology are displayed in Fig. 1, and indicate optimal ratios that are roughly 4% to 6.5% smaller than the theoretical  $\sqrt{\alpha}$  factors stated earlier. Due to the small difference in current with the skewed sizing ( $\sim 0.5\%$  to  $1.5\%$  improvement), we will use a 1:1 width ratio in stacks. This reduces the design complexity for a negligibly small performance penalty.

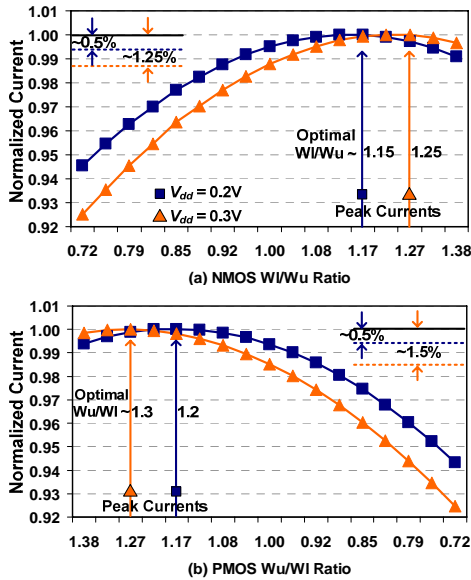


**Fig. 1.** DC current in stacks of two devices for a range of  $W_U:W_L$  sizing ratios. The total width of the stacked devices is held constant at  $1\mu\text{m}$ . The small benefits derived by using skewed stack sizing are indicated in the upper corners of the plots.

### B. Optimal 2-Stack Sizing Factor

After deciding to use a 1:1 ratio for the two devices in a stack, we must find the amount by which they should be sized up to drive the same current as a single transistor. Defining  $W = W_U = W_L$  as the size of each transistor in the stack, we can modify equation (6) as follows:

$$I_U = I_L = \frac{\alpha W^2}{\alpha W + W} e^{\frac{V_{dd} - V_{t0}}{mV_T}} = \frac{\alpha}{1 + \alpha} W e^{\frac{V_{dd} - V_{t0}}{mV_T}} \quad (9)$$

For a single transistor, the current equation is:

$$I = W_{\text{eff}} e^{\frac{V_{dd} - (V_{t0} + \lambda_d V_{dd})}{mV_T}} = \alpha W_{\text{eff}} e^{\frac{V_{dd} - V_{t0}}{mV_T}}, \quad (10)$$

where  $W_{\text{eff}}$  stands for the effective width of this device. From equations (9) and (10), we have the following relationship:

$$\alpha W_{\text{eff}} = \frac{\alpha}{1 + \alpha} W \rightarrow W_{\text{eff}} = \frac{1}{1 + \alpha} W \quad (11)$$

According to this equation, two stacked transistors should be sized up by a factor of  $(1 + \alpha)$  in relation to a single device for the same current drivability. Tables I and II display  $(1 + \alpha)$  stack sizing values from this theory and from simulation results, demonstrating the validity of equation (11). DC simulations were performed to find the correct sizing for transistors in a stack which is capable of conducting the same amount of current as a single unit-sized device. Sizing factors found in simulations were slightly smaller than those predicted by the theory derived above due to effects not captured by current equation (1), but the trend with technology scaling is nearly identical in both cases.

Results indicate that stacks need to be sized up by a larger amount in the subthreshold region compared to the strong-inversion region. Also note that NMOS stack sizing factors are significantly smaller in strong inversion due to velocity saturation.

**TABLE I**  
NMOS Stack Sizing Factors

Vdd	Sizing Method	130nm	90nm	65nm	45nm
0.2V	simulation	2.19	2.30	2.42	2.66
	theory	2.39	2.52	2.67	3.04
0.3V	simulation	2.27	2.44	2.64	3.11
	theory	2.50	2.70	2.93	3.57
1.2V	simulation	1.58	1.60	1.63	1.69

**TABLE II**  
PMOS Stack Sizing Factors

Vdd	Sizing Method	130nm	90nm	65nm	45nm
0.2V	simulation	2.33	2.48	2.68	3.00
	theory	2.45	2.66	2.90	3.34
0.3V	simulation	2.60	2.85	3.20	3.95
	theory	2.57	2.88	3.28	4.13
1.2V	simulation	1.98	2.08	2.05	2.15

## III. ARBITRARY STACK SIZES

### A. Proof of the Symmetry of the Lowest $n-1$ Device Widths in an $n$ -Stack

Building an extensive cell library based on this stack sizing framework requires an extension of our work to stacks of three or more devices. The derivation for the current equation of a three-stack, which follows a similar method as the derivation in section II.A gives us the following result:

$$I = \alpha \left[ \frac{(W_T - W_1 - W_2) W_1 W_2}{\alpha (W_T - W_1 - W_2)(W_2 + W_1) + W_1 W_2} \right] e^{\frac{V_{dd} - V_{t0}}{mV_T}} \quad (12)$$

$W_1$  and  $W_2$  stand for the widths of the two lower transistors in the stack of NMOS devices (see notation in Fig. 2).  $W_T$  is defined as  $W_T = W_1 + W_2 + W_3$ , and is used to eliminate  $W_3$ , the width of the upper device. This equation is symmetric with respect to the widths of the  $W_1$  and  $W_2$  transistors, indicating that the optimal sizes for the lower two devices in the stack are equal. We now



current. Fig. 3 displays logical effort values based on our stack sizing parameters, as well as the corresponding parasitic delay values. Parasitic delay represents the delay of a gate driving no load, and is set by the parasitic junction capacitance.

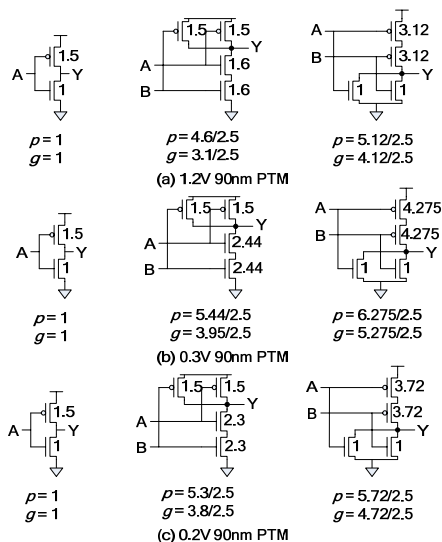


Fig. 3. Parasitic delay ( $p$ ) and logical effort ( $g$ ) values

While the additional loading on previous stages created by the larger stack sizes here can degrade the performance of some logic chains, critical paths driving substantial fanout capacitance, and particularly those containing paths dominated by stacks, do benefit from this sizing. The simple circuit illustrated in Fig. 4 is an example of a critical path whose delay is improved with our stack sizing framework. The fanout inverter widths were kept constant across all experiments, and their loading effect was taken into account through the branching factor [7]. The minimum width (i.e., the NMOS width in the unit-sized inverter) was held at  $1\mu\text{m}$ . The gate capacitance of the inverters indicated in Fig. 4 served as the input and output capacitance parameters for the logical effort calculations ( $C_{in}$  and  $C_{out}$ , respectively).

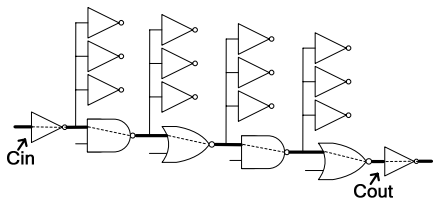


Fig. 4. Representative chain of logic gates with FO4 at each output

Delays were found for both the path through this circuit consisting entirely of stacks (the “Stacks” path), and that containing no stacks (the “Fast” path), using the worst-case input pattern for each. Critical path delay results for  $V_{dd} = 0.3\text{V}$  and  $V_{dd} = 0.2\text{V}$  are shown in Tables III and IV, respectively. As indicated here, the critical path shifts from the Stacks path to the Fast path when using the optimized subthreshold sizing, and the critical delay is consistently reduced. Also note that the  $1.2\text{V}$  sizing scheme was optimal when operating in strong-inversion, with improvements over subthreshold sizing performance ranging from  $<1\%$  to  $12.3\%$ .

In logic paths where there are not chains of stacks driving each other in sequence, the larger subthreshold stack sizing becomes less beneficial, or even detrimental in terms of performance, due

TABLE III  
Critical Path Delay Improvement for  $V_{dd} = 0.3\text{V}$

Technology	Conventional 1.2V sizing		Subthreshold 0.3V sizing	
	Delay	Crit. Path	Speedup	Crit. Path
130nm	14.86n	Stacks	7.3%	Fast
90nm	14.10n	Stacks	6.0%	Fast
65nm	16.14n	Stacks	8.1%	Fast
45nm	24.23n	Stacks	4.6%	Fast

TABLE IV  
Critical Path Delay Improvement for  $V_{dd} = 0.2\text{V}$

Technology	Conventional 1.2V sizing		Subthreshold 0.2V sizing	
	Delay	Crit. Path	Speedup	Crit. Path
130nm	98.12n	Stacks	6.6%	Fast
90nm	96.25n	Stacks	6.2%	Fast
65nm	113.8n	Stacks	8.1%	Fast
45nm	174.6n	Stacks	10.4%	Fast

to its loading effect on the previous stage. For instance, if inverters are inserted between each NAND/NOR pair in the circuit in Fig. 5, improvements in subthreshold with our larger stack sizes are reduced to  $\sim 1\%$ . In a chain of just NAND gates, the smaller stack sizes used in superthreshold were generally better choices across all supply levels. In detailed optimization schemes, care must be taken to account for transient effects, including the variance of load capacitances as operating conditions change. DC sizing schemes such as the one presented here provide us with intuition about the devices we are constructing circuits with, and a starting point for thorough optimization procedures.

## V. CONCLUSION

We have presented a new stack sizing framework for circuits operating in the subthreshold region. A closed-form solution for the optimal width ratio between different devices within a stack, as well as the sizing factor for stacked transistors was presented and shown to closely match experimental results. Our optimization scheme resulted in performance gains of up to  $10\%$  in simulations of critical paths where internal node capacitance is not dominated by the increased stack sizing factors.

## REFERENCES

- [1] A. Wang, A.P. Chandrakasan, “A 180-mV subthreshold FFT processor using a minimum energy design methodology”, *IEEE J. Solid-State Circuits*, vol. 40, no. 1, pp. 310-319, Jan. 2005.
- [2] T. Kim *et al.*, “A High-Density Subthreshold SRAM with Data Independent Bitline Leakage and Virtual Ground Replica Scheme”, *Int. Solid-State Circuits Conf.*, pp. 330-331, Feb. 2007.
- [3] C.H. Kim *et al.*, “Ultra-low-power DLMS adaptive filter for hearing aid applications”, *IEEE Transactions on VLSI Systems*, vol. 11, no. 6, pp. 1058-1067, Dec. 2003.
- [4] E. Vittoz and J. Fellrath, “CMOS analog integrated circuits based on weak inversion operations”, *IEEE J. Solid-State Circuits*, vol. 12, no. 3, pp. 224-231, June 1977.
- [5] Predictive Technology Model, online: <http://www.eas.asu.edu/~ptm/>.
- [6] W. Zhao and Y. Cao, “New generation of Predictive Technology Model for sub-45nm Design Exploration,” *Int. Symp. On Quality Electronic Design*, pp. 585-590, 2006.
- [7] I. Sutherland *et al.*, *Logical Effort: Designing Fast CMOS Circuits*. San Francisco, CA: Morgan Kaufmann, Jan. 1999.